Derivation of Volume Averaged Perturbation Equations for Aeroacoustics in Porous Materials

By B. Faßmann, J. Delfs, R. Ewert

Deutsches Zentrum für Luft- und Raumfahrt e.V.,
Institut für Aerodynamik und Strömungstechnik,
Abteilung Technische Akustik
Lielienthalplatz 7
38108 Braunschweig

The derivation of a set of volume averaged perturbation equations is presented. The new governing equations allow predicting the effect of open type porous materials on the aeroacoustics of side or trailing edges of airfoils. The numerical implementation is verified against a generic test case with homogeneous, isotropic porosity and a quiescent medium.

1. Introduction

Looking at future noise restriction of civil aircraft, the reduction of emitted noise is an important issue of present research. One important noise source of an approaching and landing aircraft is the high lift system, especially the slat and the slat cove. Alternative high lift system designs try to eliminate the slats, see [1]. Consequently, with the complete abatement of slat noise, trailing edge sound of the flap becomes the new prominent noise source.

One promising technology of reducing trailing edge sound is the installation of porous material at the trailing edge of an airfoil. Experimental investigations have shown that streamwise narrow slits perforating the rear part of an airfoil cause a broadband reduction of the emitted sound pressure level (SPL) of about 6 dB, refer to [2]. Proceeding experiments have proven the acoustic impact of isotropic porous material applied to the trailing edge. In [3], a sound reduction of the same order of magnitude is reported. Other experiments with a porous material inserted into the slat cove of a conventional high lift system has effected a 3 dB reduction of slat noise, refer to [4].

For a detailed understanding of the mechanisms which induce the acoustic benefit of porous materials to aerodynamically loaded structures, numerical simulations have certain advantages. Especially, the coupling of Computational Fluid Dynamics (CFD) and Computational Aero Acoustics (CAA) would enable complex investigation with less effort than pure experiments. Utilizing Raynolds Average Navier-Stokes (RANS) equations in the CFD step would significantly reduce computational effort compared to scale resolving simulations.

This paper presents the derivation of a set of governing equations which enable Aeroacoustic prediction in the presence of porous material, based on the method of volume averaging. The resulting equations are implemented into the DLR PIANO-Code

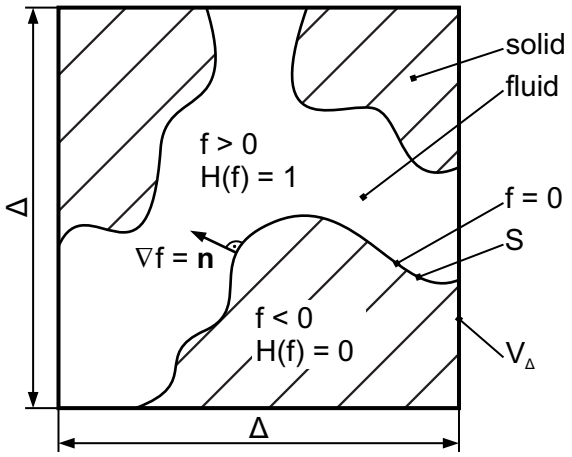

FIGURE 1. Schematic of a porous material and definition of function $f(x)$, [11].

(refer to [5]). Further, the implementation is verified against the analytical solution of a modified, inhomogeneous wave equation.

2. Volume Averaging Method

The method of volume averaging is an important tool for the numerical handling of multi-phase flows. A multi-phase system may consist of different fluids (both, gaseous or liquid) or of fluidic and solid parts. In the case of open type porosity, the two phase system is containing one fluid phase and one coherent solid phase which is which is completely flooded with the fluid phase. The subsequently following derivation restricts to this kind of porous material.

Since the late 60th, a considerable amount of work has been dedicated to the development of volume averaged conservation and transport equations, see e.g. [6–9]. Basically, the averaging operation corresponds to a spatial filtering procedure of the flow variables. The superficial volume averaging is defined as follows:

$$\langle\varphi\rangle^{\mathsf{s}}(\boldsymbol{x},t) := \frac{\int G(\boldsymbol{x}-\boldsymbol{x}',\Delta)\,\varphi^*(\boldsymbol{x}',t)d\boldsymbol{x}'}{\int G(\boldsymbol{x}-\boldsymbol{x}',\Delta)\,d\boldsymbol{x}'}\ . \tag{2.1}$$

In this expression, G denotes a spatial filter function. The filter is centered at $\boldsymbol{x}$ and has a fixed extension defined by length scale Δ, i.e. it decays to zero for $|\boldsymbol{x}-\boldsymbol{x}'| >> \Delta$. For example, the filter could be chosen to be a Gaussian with standard deviation Δ.

The quantity φ^* denotes a generalized variable which is well defined in the entire volume, i.e. in the porous volume as well as in the solid phase of a porous material. It is given by

$$\varphi^*(\boldsymbol{x},t) = \varphi(\boldsymbol{x},t)H(f(\boldsymbol{x}))\ . \tag{2.2}$$

Here, H denotes the Heaviside-function. It depends on $f(\boldsymbol{x})$ which is a function defined to be $f<0$ in the solid material and $f>0$ in the fluid, i.e. $f=0$ indicates the surface between solid and fluid inside the porous medium, refer to Fig. 1. The gradient of $f(0)$ is normal to the interface surfaces. Without losing generality, the scaling of f is defined such that the gradient is the wall normal unity vector and points into the fluid phase, i.e. $\boldsymbol{\nabla} f = \boldsymbol{n}$. For further details regarding generalized variables and their application

refer to [10]. The integrals (without explicitly specified bounds) are taken over the entire space. In general, the integral over the filter kernel defines a characteristic filter volume,

$$V_\Delta = \int G\left(\boldsymbol{x}-\boldsymbol{x}',\Delta\right) d^3x' \ . \tag{2.3}$$

The intrinsic averaged variable is defined by

$$\langle\varphi\rangle^{\mathsf{i}}\left(\boldsymbol{x},t\right) := \frac{\int G\left(\boldsymbol{x}-\boldsymbol{x}',\Delta\right)\varphi^*(\boldsymbol{x}',t)d^3x'}{\int G\left(\boldsymbol{x}-\boldsymbol{x}',\Delta\right)H(f(\boldsymbol{x}'))d^3x'} \ . \tag{2.4}$$

From now on, $\langle\varphi\rangle^{\mathsf{i}}$ will be expressed as $\langle\varphi\rangle$. We can define a porosity factor $\bar{\phi}$ via

$$\bar{\phi} = \frac{\int G\left(\boldsymbol{x}-\boldsymbol{x}',\Delta\right)H(f(\boldsymbol{x}'))d^3x'}{\int G\left(\boldsymbol{x}-\boldsymbol{x}',\Delta\right)d^3x'}, \tag{2.5}$$

which, based on the definitions Eqs. (2.1) and (2.4) for intrinsic and superficial averaged quantities, yields the following generally valid relationship between both volume averaged quantities:

$$\langle\varphi\rangle^{\mathsf{s}} = \bar{\phi}\ \langle\varphi\rangle \ . \tag{2.6}$$

It always is $0 \leq \bar{\phi} \leq 1$, where $\bar{\phi} = 1$ in free fluid and $\bar{\phi} = 0$ represents a solid body. In the special case where the filter kernel is chosen to be a discontinuous top-hat function $G(\boldsymbol{x}-\boldsymbol{x}',\Delta) = g(x-x')g(y-y')g(z-z')$, where $g(x)$ is defined by

$$g(x) = 1 - H\left(|x| - \Delta/2\right) \ , \tag{2.7}$$

the superficial averaged variable reads

$$\langle\varphi\rangle^{\mathsf{s}} = \frac{1}{V_\Delta}\int_{V_F}\varphi d^3x' \ . \tag{2.8}$$

The top-hat function restricts the integration volume to a finite extension $V_\Delta = \Delta^3$ centered at the given position (window averaging). V_F is the fluid volume of the porous material inside the actual window; it satisfies $V_F = \bar{\phi}V$. The intrinsic volume averaged variable in this case becomes

$$\langle\varphi\rangle = \frac{1}{V_F}\int_{V_F}\varphi d^3x' \ . \tag{2.9}$$

Let us consider the density ρ to be the quantity of interest. For a point inside the fluid phase the intrinsic density becomes in the limit $\Delta \to 0$ equal to the local density in the fluid, i.e.

$$\langle\rho\rangle\left(\boldsymbol{x},t\right) \to \rho(\boldsymbol{x},t) \quad \text{for} \quad \Delta \to 0 \ . \tag{2.10}$$

In order to smooth out geometrical details of the porous medium, such that the volume averaged variables become continuous over the porous material, a length scale $\Delta > D_p$ must be used, where D_p denotes a length scale derived from a characteristic pore size. In this case, the intrinsic volume averaged density has the same order of magnitude as a local density, it is, however, a quantity defined over the entire space, which moreover can be spatially differentiated if a continuous filter function G is applied. The superficial averaged density is smaller as defined by the porosity parameter $\bar{\phi}$. Hence, at interfaces between porous materials and free fluid the intrinsic density will only exhibit a gradual change over the interface, whereas the superficial averaged density will change rapidly over a scale Δ. Inside a homogeneous porous material, the explicit value of $\bar{\phi}$ will be

independent for sufficient large Δ from the explicit chosen length scale in Eq. (2.5). However, at an interface between the porous medium and a free fluid, $\bar{\phi}$ will change gradually over a length Δ from its value in the porous medium to one inside the fluid phase.

Favre volume averaged velocities are defined via

$$[v_i] = [v_i]^{\mathsf{i}} = \frac{\langle \rho v_i \rangle}{\langle \rho \rangle} \equiv \frac{\langle \rho v_i \rangle^{\mathsf{s}}}{\langle \rho \rangle^{\mathsf{s}}} = [v_i]^{\mathsf{s}} \ . \tag{2.11}$$

To derive volume averaged perturbation equations, the Navier-Stokes equations in conservative notation are superficially volume averaged assuming the application of a spatial differentiable filter $G(|\boldsymbol{x}-\boldsymbol{x}'|)$. In the fluid ($\bar{\Phi}=1$) the resulting equations correspond to those used for large eddy simulation (LES), i.e. they formally correspond to the Navier-Stokes equations for volume averaged variables plus some extra subgrid scale stress terms on the right-hand side.

During derivation, commutation of volume averaging and differentiation is applied. Following the definition Eq. (2.1), for the temporal and spatial derivatives of a quantity φ it follows

$$\left\langle \frac{\partial \varphi}{\partial t} \right\rangle^{\mathsf{s}} = \frac{\partial}{\partial t} \langle \varphi \rangle^{\mathsf{s}} \text{ and } \left\langle \frac{\partial \varphi}{\partial x_i} \right\rangle^{\mathsf{s}} = \frac{\partial \langle \varphi \rangle^{\mathsf{s}}}{\partial x_i} - \frac{1}{V_\Delta} \int_S G\, \varphi n_i \, dS \ . \tag{2.12}$$

The derivation is shown in more detail in [11].

2.1. *Independent variables*

For numerical stability reasons, the independent variables finally used for a reformulation of volume averaged governing equations are selected based on the prerequisite to be (almost) continuous across an interface between fluid and the porous medium. This way, gradients that occur inevitably due to the sudden jump of porosity across the boundary can be lumped together in extra terms linear in the used independent variables which resemble a numerically resolved localized function with a distinct peak across the interface. If applied in conjunction with explicit time integration, these extra terms could trigger numerical instabilities. To circumvent this problem, their contribution can be treated implicitly in a mixed implicit-explicit time integration method (IMEX methods, refer to [12,13]), whereas all spatial gradient terms occurring in the governing equations can be treated further on by means of explicit time integration. Since the extra terms are localized, i.e. proportional to the fluctuating variables and do not involve information from neighbor nodes of the computational mesh, implicit treatment in the framework of SDIRK methods (see [12]) demands only for inversion of an $n \times n$ matrix (depending on the dimension n of the problem) composed out of steady mean-flow variables, which is computed and stored at the begin of an unsteady simulation cycle. Therefore, highly efficient treatment of these implicit gradient terms becomes feasible.

To discuss further the appropriate choice of independent variables, we consider a test set-up of an incompressible channel flow in which a zone of porosity is applied across the channel, refer to Fig. 2. For this case, the intrinsic density in the porous medium, where $0 < \bar{\phi} < 1$ holds, is a constant quantity, since

$$\langle \rho \rangle = \frac{\int GH\rho \mathrm{d}^3x}{\int GH \mathrm{d}^3x} = \frac{\rho \int GH \mathrm{d}^3x}{\int GH \mathrm{d}^3x} = \rho \ . \tag{2.13}$$

Mass conservation across the bulk and in the porosity implies $\rho u = \langle \rho \rangle^s [u] = \mathrm{const}$.

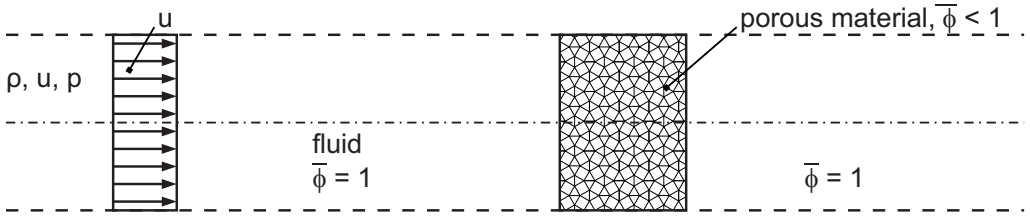

FIGURE 2. Sketch of a channel flow with porous blocking, [11].

Using Eq. (2.13) and with the help of Eq. (2.6) this yields $u = \bar{\phi}\,[u]$. Hence, to accomplish almost continuous variables across the fluid-porous interface, we introduce a new velocity variable defined by $\hat{v}_i := \bar{\phi}\,[v_i]$. Furthermore, we chose the intrinsic volume-averaged fluctuating density $\langle\rho\rangle$ and the intrinsic volume-averaged fluctuating pressure $\langle p\rangle$ to close the set of independent variables.

3. Volume Averaged Governing Equations

In this section, the governing equations of the acoustic fluctuations will be derived. First, the conservative form of the Navier-Stokes-Equations (NS Equations) is volume averaged. In a next step, the usual Euler assumptions will be made to derive the Linearized Euler Equations (LEE) in perturbation form. From this set of equations, the Linearized Perturbation Equations (LPE) will finally be deduced.

3.1. *Navier Stokes Equations*

The starting point of the derivation of a set of volume averaged governing equations for a porous material is the set of NS equations in conservation formulation

$$\frac{\partial \rho}{\partial t} + \frac{\partial \rho v_i}{\partial x_i} = 0 \tag{3.1}$$

$$\frac{\partial \rho v_i}{\partial t} + \frac{\partial \rho v_i v_j}{\partial x_j} + \frac{\partial p}{\partial x_i} - \frac{\partial \tau_{ij}}{\partial x_j} = 0 \tag{3.2}$$

$$\frac{\partial \rho e_\mathrm{t}}{\partial t} + \frac{\partial \rho e_\mathrm{t} v_i}{\partial x_i} + \frac{\partial p v_i}{\partial x_i} + \frac{\partial q_i}{\partial x_i} - \frac{\partial \tau_{ij} v_j}{\partial x_i} = 0 \tag{3.3}$$

It is Eq. (3.1) the conservation of mass, Eq. (3.2) the conservation of momentum and Eq. (3.3) the conservation of energy. The tensor $\tau_{ij} = \mu\,(\partial v_i/\partial x_j + \partial v_j/\partial x_i - 2/3\;\partial v_k/\partial x_k\;\delta_{ij})$ describes the viscous shear stress and it is μ the dynamic viscosity. Further it is $q_i = -k\;\partial T/\partial x_i$ the thermal diffusion with k the thermal conductivity. In addition, a thermally and calorically ideal gas is assumed. Thus, the total energy e_t is $\rho e_\mathrm{t} = p/\gamma-1 + \rho/2\;v_i^2$, while γ is the isotropic exponent and it is $v_i^2 = v_i v_i = v_1^2 + v_2^2 + v_3^2$, refer to [14].

Volume averaging of the Eq. (3.1) yields

$$\left\langle \frac{\partial \rho}{\partial t} \right\rangle^\mathsf{s} + \left\langle \frac{\partial \rho v_i}{\partial x_i} \right\rangle^\mathsf{s} = 0\,, \tag{3.4}$$

where superficial averaging was chosen to keep commutativity of volume averaging and differentiation. Application of Eqs. (2.11) and (2.12) leads to

$$\frac{\partial \langle\rho\rangle^\mathsf{s}}{\partial t} + \frac{\partial \langle\rho\rangle^\mathsf{s}\,[v_i]}{\partial x_i} - \frac{1}{V_\Delta}\int_S G\,\rho\,v_i n_i\;dS = 0\,. \tag{3.5}$$

The integral expression vanishes due to the no-slip condition of the velocity at the wall. Switching to intrinsic volume average $\langle\varphi\rangle^{\mathsf{s}} = \phi\,\langle\varphi\rangle$ with $\phi \neq f(t)$ and application of the continuous velocity variable $\hat{v}_i = \phi\,[v_i]$, the continuity equation of the volume averaged NS equations finally is

$$\frac{\partial\langle\rho\rangle}{\partial t} + \frac{1}{\phi}\frac{\partial\langle\rho\rangle\,\hat{v}_i}{\partial x_i} = 0 \tag{3.6}$$

The superficial volume averaging of Eq. (3.2) yields

$$\left\langle\frac{\partial\rho v_i}{\partial t}\right\rangle^{\mathsf{s}} + \left\langle\frac{\partial\rho v_i v_j}{\partial x_j}\right\rangle^{\mathsf{s}} + \left\langle\frac{\partial p}{\partial x_i}\right\rangle^{\mathsf{s}} - \left\langle\frac{\partial\tau_{ij}}{\partial x_j}\right\rangle^{\mathsf{s}} = 0 \tag{3.7}$$

Now, the definition $\langle\rho v_i v_j\rangle^{\mathsf{s}} = \langle\rho\rangle^{\mathsf{s}}\,[v_i]\,[v_j] + \left(\langle\rho v_i v_j\rangle^{\mathsf{s}} - \langle\rho\rangle^{\mathsf{s}}\,[v_i]\,[v_j]\right)$ is introduced. Further, Favre volume averaged velocities are used and the commutativity of superficial volume averaging and differentiation is applied, knowing the normal velocity component at the wall to be equal to zero. This yields

$$\begin{aligned}\frac{\partial\langle\rho\rangle^{\mathsf{s}}\,[v_i]}{\partial t} + \frac{\partial}{\partial x_j}\left(\langle\rho\rangle^{\mathsf{s}}\,[v_i]\,[v_j]\right) + \frac{\partial\langle p\rangle^{\mathsf{s}}}{\partial x_i} - \frac{\partial\langle\tau_{ij}\rangle^{\mathsf{s}}}{\partial x_j}& \\ + \frac{\partial}{\partial x_j}\left(\langle\rho v_i v_j\rangle^{\mathsf{s}} - \langle\rho\rangle^{\mathsf{s}}\,[v_i]\,[v_j]\right)& \\ - \frac{1}{V_\Delta}\int_S G\,p n_i\,\mathrm{d}S + \frac{1}{V_\Delta}\int_S G\,\tau_{ij} n_i\,\mathrm{d}S = 0\,.&\end{aligned} \tag{3.8}$$

The last three terms of the LHS are replaced by the expression

$$\underbrace{\frac{\partial}{\partial x_j}\left(\langle\rho v_i v_j\rangle^{\mathsf{s}} - \langle\rho\rangle^{\mathsf{s}}\,[v_i]\,[v_j]\right)}_{\text{subfilter stresses}} \underbrace{- \frac{1}{V_\Delta}\int_S G\,p n_i\,\mathrm{d}S + \frac{1}{V_\Delta}\int_S G\,\tau_{ij} n_i\,\mathrm{d}S}_{\text{porous drag}} =: \mathcal{F}_i\,. \tag{3.9}$$

Reformulating this equation with primitive variable leads to

$$\frac{\partial[v_i]}{\partial t} + [v_j]\,\frac{\partial[v_i]}{\partial x_j} + \frac{1}{\langle\rho\rangle^{\mathsf{s}}}\frac{\partial\langle p\rangle^{\mathsf{s}}}{\partial x_i} - \frac{1}{\langle\rho\rangle^{\mathsf{s}}}\frac{\partial\langle\tau_{ij}\rangle^{\mathsf{s}}}{\partial x_j} + \frac{1}{\langle\rho\rangle^{\mathsf{s}}}\mathcal{F}_i = 0\,. \tag{3.10}$$

The additional term $\mathcal{F}_i$ can be expressed via the combination of the Darcy term and the Forchheimer term (see [11]), namely

$$\frac{1}{\langle\rho\rangle^{\mathsf{s}}}\mathcal{F}_i = \underbrace{\phi\frac{\langle\nu\rangle^{\mathsf{s}}}{\kappa}[v_i]}_{\text{Darcy term}} + \underbrace{\langle\rho\rangle^{\mathsf{s}}\,\phi^2\frac{c_{\mathsf{F}}}{\sqrt{\kappa}}\sqrt{[v_k][v_k]}[v_i]}_{\text{Forchheimer term}}\,. \tag{3.11}$$

The model parameters are κ, the permeability and c_{F}, the empiric Forchheimer constant. Further, it is ν the kinematic viscosity. Switching to intrinsic volume average $\langle\varphi\rangle^{\mathsf{s}} = \phi\,\langle\varphi\rangle$ with $\phi \neq f(t)$ and application of the continuous velocity variable $\hat{v}_i = \phi\,[v_i]$, the momentum equation of the volume averaged NS equations finally is

$$\begin{aligned}\frac{\partial\hat{v}_i}{\partial t} + \frac{1}{\phi}\hat{v}_j\frac{\partial\hat{v}_i}{\partial x_j} + \frac{\phi}{\langle\rho\rangle}\frac{\partial\langle p\rangle}{\partial x_i} - \frac{\phi}{\langle\rho\rangle}\frac{\partial\langle\tau_{ij}\rangle}{\partial x_j}& \\ + \phi\frac{\langle\nu\rangle}{\kappa}\hat{v}_i + \phi\frac{c_{\mathsf{F}}}{\sqrt{\kappa}}\sqrt{\hat{v}_k\hat{v}_k}\hat{v}_i& \\ + \left[\hat{v}_i\hat{v}_j + \phi^2\frac{\langle\tau_{ij}\rangle}{\langle\rho\rangle}\right]\frac{\partial}{\partial x_j}\frac{1}{\phi} - \phi^2\frac{\langle p\rangle}{\langle\rho\rangle}\frac{\partial}{\partial x_i}\frac{1}{\phi} = 0\,.&\end{aligned} \tag{3.12}$$

To separate the porosity ϕ from the flow quantities via chain rule, it was used the relationship $\phi^{-1}\ {}^{\partial\phi}/_{\partial x_i} = -\phi\ {}^{\partial\phi^{-1}}/_{\partial x_i}$.

The superficial volume average of the energy equation Eq. (3.3) can be expressed by

$$\frac{\partial\langle\rho e\rangle^{\mathsf{s}}}{\partial t} + \frac{\partial\langle\rho h v_i\rangle^{\mathsf{s}}}{\partial x_i} + \frac{1}{2}\frac{\partial\langle v_i v_j^2\rangle^{\mathsf{s}}}{\partial x_i} + \frac{\partial\langle q_i\rangle^{\mathsf{s}}}{\partial x_i} - \frac{\partial\langle\tau_{ij} v_j\rangle^{\mathsf{s}}}{\partial x_i} - \frac{1}{V_\Delta}\int_S G\, q_i n_i \,\mathrm{d}S = 0\,, \quad (3.13)$$

while the normal velocity component at the wall is equal to zero. The symbol h denotes the specific enthalpy and it is

$$h = \frac{\gamma}{\gamma-1}\frac{p}{\rho} \qquad \Leftrightarrow \qquad p = \frac{\gamma-1}{\gamma}\rho h \quad (3.14)$$

By application of the definition of e_t and addition of $-\left\langle {}^{v_j^2}/_2 \cdot \text{Eq. (3.1)}\right\rangle^{\mathsf{s}}$, the first term of Eq. (3.13) may be reformulated,

$$\frac{\partial\langle\rho e_\mathrm{t}\rangle^{\mathsf{s}}}{\partial t} = \frac{1}{\gamma-1}\frac{\partial\langle p\rangle^{\mathsf{s}}}{\partial t} + \left\langle v_j\frac{\partial\rho v_j}{\partial t}\right\rangle^{\mathsf{s}} + \left\langle v_j\frac{\partial\rho v_i v_j}{\partial x_i}\right\rangle^{\mathsf{s}} - \frac{1}{2}\frac{\partial}{\partial x_i}\left\langle\rho v_i v_j^2\right\rangle^{\mathsf{s}}\,. \quad (3.15)$$

The second term of Eq. (3.13) can be expressed as

$$\frac{\partial\langle\rho h v_i\rangle^{\mathsf{s}}}{\partial x_i} = \frac{\partial}{\partial x_i}\langle\rho\rangle^{\mathsf{s}}[h][v_i] + \frac{\partial}{\partial x_i}\left(\langle\rho h v_i\rangle^{\mathsf{s}} - \langle\rho\rangle^{\mathsf{s}}[h][v_i]\right)\,. \quad (3.16)$$

In the next step, the expression $-\langle v_i \cdot \text{Eq. (3.2)}\rangle^{\mathsf{s}}$ will be prepared with careful permutation of the indices i and j. This yields

$$-\left\langle v_j\frac{\partial\rho v_j}{\partial t}\right\rangle^{\mathsf{s}} - \left\langle v_j\frac{\partial\rho v_i v_j}{\partial x_i}\right\rangle^{\mathsf{s}} - \left\langle v_i\frac{\partial p}{\partial x_i}\right\rangle^{\mathsf{s}} + \left\langle\frac{\partial v_j\tau_{ij}}{\partial x_i}\right\rangle^{\mathsf{s}} - \left\langle\tau_{ij}\frac{\partial v_j}{\partial x_i}\right\rangle^{\mathsf{s}} = 0\,. \quad (3.17)$$

Now, the Eqs. (3.14) to (3.16) will be inserted and Eq. (3.17) is added to Eq. (3.13). Then, the energy equation can be expressed in terms of pressure p. It is

$$\begin{aligned}
&\frac{\partial\langle p\rangle^{\mathsf{s}}}{\partial t} + [v_i]\frac{\partial\langle p\rangle^{\mathsf{s}}}{\partial x_i} + \gamma\langle p\rangle^{\mathsf{s}}\frac{\partial[v_i]}{\partial x_i} \\
&\quad - (\gamma-1)\left(\langle\tau_{ij}\rangle^{\mathsf{s}}\frac{\partial[v_j]}{\partial x_i} + \frac{\partial\langle q_i\rangle^{\mathsf{s}}}{\partial x_i} - \frac{1}{V_\Delta}\int_S G\, q_i n_i \,\mathrm{d}S\right) \\
&\quad - (\gamma-1)\left(\left\langle\tau_{ij}\frac{\partial v_j}{\partial x_i}\right\rangle^{\mathsf{s}} - \langle\tau_{ij}\rangle^{\mathsf{s}}\frac{\partial[v_j]}{\partial x_i}\right) \\
&\quad + (\gamma-1)\left(\left\langle p\frac{\partial v_i}{\partial x_i}\right\rangle^{\mathsf{s}} - \langle p\rangle^{\mathsf{s}}\frac{\partial[v_i]}{\partial x_i}\right) \\
&\quad + \frac{\gamma-1}{\gamma}\frac{\partial}{\partial x_i}\left(\langle\rho h v_i\rangle^{\mathsf{s}} - \langle\rho\rangle^{\mathsf{s}}[h][v_i]\right) = 0\,.
\end{aligned} \quad (3.18)$$

The last three terms of the LHS may be neglected. Switching to intrinsic volume average $\langle\varphi\rangle^{\mathsf{s}} = \phi\langle\varphi\rangle$ with $\phi \neq f(t)$ and application of the continuous velocity variable $\hat{v}_i = \phi[v_i]$,

the energy equation of the volume averaged NS equations finally is

$$\begin{aligned}
&\frac{\partial\langle p\rangle}{\partial t}+\frac{1}{\phi}\left(\hat{v}_j\frac{\partial\langle p\rangle}{\partial x_j}+\gamma\,\langle p\rangle\,\frac{\partial\hat{v}_j}{\partial x_j}\right)\\
&\quad+(\gamma-1)\left(-\frac{\langle\tau_{ij}\rangle}{\phi}\frac{\partial\hat{v}_i}{\partial x_j}+\frac{\partial\langle q_i\rangle}{\partial x_i}-\frac{1}{\phi V_\Delta}\int_S G\,q_i n_i\,\mathrm{d}S\right)\\
&\quad+(\gamma-1)\left[\left(\langle p\rangle\,\hat{v}_j-\langle\tau_{ij}\rangle\,\hat{v}_i\right)\frac{\partial}{\partial x_j}\left(\frac{1}{\phi}\right)-\phi\,\langle q_i\rangle\,\frac{\partial}{\partial x_i}\left(\frac{1}{\phi}\right)\right]=0\,.
\end{aligned}\tag{3.19}$$

3.2. *Linearized Euler Equations*

For the derivation of volume averaged LEE, we decompose the volume averaged pressure and density into a mean, i.e. time-averaged ($\overline{\varphi}$), and a fluctuating part (φ'). Let φ now indicate density or pressure, i.e. $\varphi\in\{\rho,p\}$, then the decomposition reads

$$\langle\varphi\rangle^{\mathsf{s}}=\overline{\langle\varphi\rangle^{\mathsf{s}}}+\langle\varphi\rangle^{\mathsf{s}\prime}\ \text{with}\overline{\varphi}=\lim_{\Delta t\to\infty}\int_{t_0}^{t_0+\Delta t}\varphi\,\mathrm{d}t\,.\tag{3.20}$$

The Favre volume averaged velocity defined by Eq. (2.11) is decomposed into a Favre averaged mean-part plus a fluctuation, i.e.

$$[v_i]=\widetilde{[v_i]}+[v_i]''\ \text{with}\widetilde{[v_i]}:=\frac{\overline{\langle\rho\rangle^{\mathsf{s}}\,[v_i]}}{\overline{\langle\rho\rangle}}\,,\tag{3.21}$$

where the bar indicating a time average part from Eq. (3.20). It is easy to prove that Favre averaging applied to volume averaged quantities still satisfies the usual relations

$$\overline{\langle\rho\rangle\,[v_i]''}=0\tag{3.22}$$

and

$$\overline{\langle\rho\rangle^{\mathsf{s}}\,[v_i]\,[v_j]}=\langle\rho\rangle^{\mathsf{s}}\,\widetilde{[v_i]}\widetilde{[v_j]}+\overline{\langle\rho\rangle^{\mathsf{s}}\,[v_i]''\,[v_j]''}\,.\tag{3.23}$$

Remind, superficial volume averaging for density and pressure must have been applied to the volume averaged Navier-Stokes equations to enable their reformulation in conservative notation that eventually can be transformed into a formulation based on primitive volume averaged variables, refer to Section 3.1. For the desired set of continuous, independent variables based on intrinsic volume averaged density and pressure as well as on the velocity $\hat{v}_i$, in a final step the variables were substituted accordingly. Introduction of the above presented variable decomposition and linearization allows to derive volume averaged LEE in terms of independent variables $\left(\langle\rho\rangle',\hat{v}_i'',\langle p\rangle'\right)$. To simplify the syntax, subsequently a notation without additional brackets to indicate intrinsic volume averaged quantities will be used. Then the substitutions

$$\rho'\to\langle\rho\rangle'\ ,\quad \rho^0\to\overline{\langle\rho\rangle}\ ,\quad p'\to\langle p\rangle'\ ,\quad p^0\to\overline{\langle p\rangle}\ ,\quad \hat{v}_i{}'\to\hat{v}_i{}''\quad\text{and}\quad \hat{v}_i{}^0\to\widetilde{\hat{v}_i}\tag{3.24}$$

will by applied to eventually reformulate the volume averaged LEE. Furthermore, a simplified notation is introduced for convenience by omitting the overbar on ϕ, i.e. $\overline{\phi}\to\phi$, as the porosity ϕ is temporally independent.

The next step of the derivation of the volume averaged LEE involves neglecting all viscous terms except for the Darcy and Forchheimer model terms, i.e. $\tau_{ij}=0$. Further, heat conduction is omitted, since it is of less relevance in the context of acoustics, see [14], i.e. $q_i=0$. By means of Eqs. (3.20) and (3.21), the flow quantities will be separated

into mean and perturbed parts. Nonlinear perturbation contributions will be neglected in the sense of linearization. The continuity equation of the LEE finally reads

$$\frac{\partial \rho'}{\partial t} + \frac{1}{\phi}\left(\hat{v}_i^0 \frac{\partial \rho'}{\partial x_i} + \hat{v}_i' \frac{\partial \rho^0}{\partial x_i} + \rho^0 \frac{\partial \hat{v}_i'}{\partial x_i} + \rho' \frac{\partial \hat{v}_i^0}{\partial x_i}\right) = 0 \,. \tag{3.25}$$

The following estimates will be relevant in the linearization procedure of the momentum equation:

$$\frac{\varphi'}{\phi^0 + \varphi'} \approx \frac{\varphi'}{\phi^0} \text{ for } \varphi \ll 1 \,. \tag{3.26}$$

$$(1+\varphi')^n \approx 1 + n\varphi \text{ for } \varphi \ll 1 \,. \tag{3.27}$$

Further, it is assumed to be

$$p' = c_0^2 \rho' \text{ with} c_0^2 = \frac{\gamma p^0}{\rho^0} \tag{3.28}$$

for the volume averaged quantities, while it is c_0 the speed of sound in the free fluid†. The momentum equation of the LEE finally reads

$$\begin{aligned} &\frac{\partial \hat{v}_i'}{\partial t} + \frac{1}{\phi}\left[\hat{v}_j{}^0 \frac{\partial \hat{v}_i'}{\partial x_j} + \hat{v}_j{}' \frac{\partial \hat{v}_i^0}{\partial x_j}\right] + \frac{\phi}{\rho^0}\left[\frac{\partial p'}{\partial x_i} - \frac{\rho'}{\rho^0}\frac{\partial p^0}{\partial x_i}\right] \\ &\quad \underbrace{+ \phi \frac{\nu}{\kappa}\delta_{ij}\hat{v}_j' + \phi \frac{c_\mathsf{F}}{\sqrt{\kappa}}\sqrt{\hat{v}_k^0 \hat{v}_k^0}\left[e_i^0 e_j^0 + \delta_{ij}\right]\hat{v}_j'}_{\text{model terms Darcy and Forchheimer}} \\ &\quad + \hat{v}_j'\left(\hat{v}_i^0 \frac{\partial}{\partial x_j}\frac{1}{\phi} + \delta_{ij}\hat{v}_k^0 \frac{\partial}{\partial x_k}\frac{1}{\phi}\right) - p' \frac{\phi^2}{\rho^0}\frac{\gamma - 1}{\gamma}\frac{\partial}{\partial x_i}\frac{1}{\phi} = 0 \,, \end{aligned} \tag{3.29}$$

where it is $\hat{v}_k^0 / \sqrt{\hat{v}_j^{0\,2}} =: e_k^0$.

The linearization of the energy equation finally yields

$$\begin{aligned} &\frac{\partial p'}{\partial t} + \frac{1}{\phi}\left(\hat{v}_i^0 \frac{\partial p'}{\partial x_i} + \hat{v}_i' \frac{\partial p^0}{\partial x_i}\right) + \frac{\gamma}{\phi}\left(p^0 \frac{\partial \hat{v}_i'}{\partial x_i} + p' \frac{\partial \hat{v}_i^0}{\partial x_i}\right) \\ &\quad + (\gamma - 1)\left(p^0 \hat{v}_i' + p' \hat{v}_i^0\right) \frac{\partial}{\partial x_i}\frac{1}{\phi} = 0 \end{aligned} \tag{3.30}$$

Now, the set of volume averaged LEE is complete. Besides the model terms in the momentum equations representing the effect of the solid phase on the fluid, some gradient terms of the inverted porosity ϕ^{-1} occur. These terms have physical reasons as the spatial filter function G is shifted continuously, even across the edge between free fluid and porous material. For a numerical realization, the additional model terms need for smoothing out jumps in the spatial distribution of porosity ϕ, permeability κ and Forchheimer constant c_F.

3.3. *Linearized Perturbation Equations*

The volume averaged LPE differ from the LEE only in the momentum equation. Continuity equation Eq. (3.25) and energy equation Eq. (3.30) remain the same. Unlike the LEE, the LPE do not resolve vorticity modes. On the contrary, the LPE need for source terms modeling the local vorticity fluctuations. Thus, the second and third term of Eq. (3.29)

† The sound propagation in the porous material is dispersive, i.e. the phase and the group velocity differ. Please refer to [11].

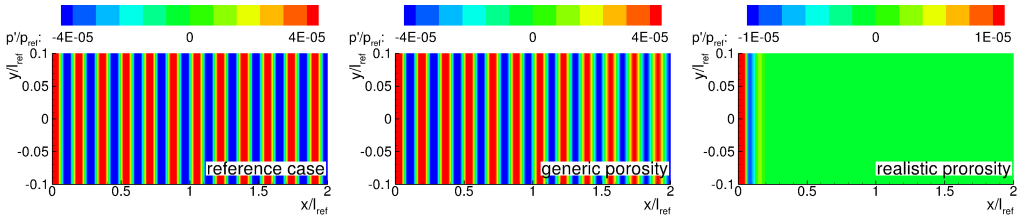

FIGURE 3. Snapshot of the acoustic response to a harmonic plane wave front at 2 kHz for three different isotropic, homogeneously porous materials; (left) free medium as a reference, (middle) generic porosity and (right) realistic porosity. The reference pressure is $p_{\text{ref}} = \rho^0 c_0^2$ and the reference length is $l_{\text{ref}} = 1\,\text{m}$.

may be rewritten as

$$\frac{1}{\phi}\left(\left(\hat{v}_j^0 \frac{\partial}{\partial x_j}\hat{v}_i'\right) + \left(\hat{v}_j' \frac{\partial}{\partial x_j}\hat{v}_i^0\right)\right) = \frac{1}{\phi}\left(\frac{\partial}{\partial x_i}\left(\hat{v}_k^0 \hat{v}_k'\right) - S_{v,i}\right) . \tag{3.31}$$

The RHS source term $-S_{v,i}$ contains the vorticity modes. In the next step of derivation of the complete set of the LPE, we take advantage from Eq. (3.28). The momentum equation finally reads

$$\begin{aligned}
&\frac{\partial \hat{v}_i'}{\partial t} + \frac{1}{\phi}\frac{\partial \hat{v}_k^0 \hat{v}_k'}{\partial x_i} + \phi \frac{\partial}{\partial x_i}\left(\frac{p'}{\rho^0}\right) + \\
&\quad + \phi \frac{\nu}{\kappa}\delta_{ij}\hat{v}_j' + \phi \frac{c_{\mathsf{F}}}{\sqrt{\kappa}}\sqrt{\hat{v}_k^0 \hat{v}_k^0}\left[e_i^0 e_j^0 + \delta_{ij}\right]\hat{v}_j' + \\
&\quad + \left(\hat{v}_i^0 \frac{\partial}{\partial x_j}\frac{1}{\phi} + \delta_{ij}\hat{v}_k^0 \frac{\partial}{\partial x_k}\frac{1}{\phi}\right)\hat{v}_j' - p' \frac{\phi^2}{\rho^0}\frac{\gamma - 1}{\gamma}\frac{\partial}{\partial x_i}\frac{1}{\phi} \\
&\quad = S_{v,i} - \frac{\phi}{\rho^{0\,2}}\left(\frac{\partial \rho^0 p'}{\partial x_i} - \frac{\partial \rho' p^0}{\partial x_i}\right) + \frac{\phi}{\rho^0}\left((1-\gamma)\frac{\partial p'}{\partial x_i} + \frac{\rho'}{\gamma}\frac{\partial a_0^2}{\partial x_i}\right) .
\end{aligned} \tag{3.32}$$

The last term of the RHS represent entropy fluctuations and may be neglected.

4. Verification

As a simple verification test case for the implementation of the porous terms, the wave propagation in a quiescent medium is studied for different porous materials. The results are taken from [11]. Two different isotropic porosities were chosen: A generic one with artificially chosen porosity parameters and a realistic one with parameters deduced from measurements. The realistic case is based on sintered metals fiber felt. The 2-D-computational domain has an extension of $x = -1\,\text{m} \ldots +1\,\text{m}$ and $y = -0.5\,\text{m} \ldots 0.5\,\text{m}$. The fluid phase is ambient air considered as an ideal gas with properties $c_0 = 343\,\text{m/s}$, $p^0 = 1.01325 \cdot 10^5\,\text{Pa}$ and $\rho^0 = 1.205\,\text{kg/m}^3$. The grid is designed to resolve frequencies up to $f = 20\,\text{kHz}$. No additional background damping was used.

For the first test case with isotropic porosity and a quiescent medium, mono-frequent incoming plane waves with different frequencies were specified at the left boundary through a Thompson boundary condition, refer to [15, 16]. In Fig. 3, a snap shot of the acoustic response is shown for a harmonic signal at $2\,\text{kHz}$. For quantitative evaluation, signals were picked from a horizontal line at $y = 0.1\,\text{m}$.

For a medium at rest, the theoretical damping envelope can be derived from the 1-D wave equation. The damping can be reduced to the ratio of the local root mean square

value $\tilde{p}$ of the sound pressure p' to its maximal value at the position $p'_{\mathsf{max}}(x_s)$ of the source, i.e. $\tilde{p}^2 = \overline{(p')^2}$. Considering a homogeneous, isotropic porosity, the damping envelope with respect to x results from:

$$\frac{\tilde{p}(x)}{\tilde{p}_{\mathsf{max}}} = \exp\left(-\frac{\omega}{c_0}\sqrt{\frac{1}{2}\sqrt{\frac{(\phi\,\nu\,\kappa^{-1})^2}{\omega^2}+1}-\frac{1}{2}}\;x\right) =: \exp(\lambda^{(\mathsf{D,sim})}x)\;. \tag{4.1}$$

While the exponent (D) denotes the analytical damping behavior, the exponent (sim) indicates the damping behavior predicted by the simulation. Further, it is L_{p} the sound pressure level of $\tilde{p}$. Namely it is

$$L_{\mathsf{p}}^{(\mathsf{D,sim})}(x) = 20\log\left(\frac{\tilde{p}(x)}{\tilde{p}_{\mathsf{max}}}\right) = \frac{20}{\ln(10)}\lambda^{(\mathsf{D,sim})}x\;. \tag{4.2}$$

Finally, the degree of agreement between the analytical result and the computiation can be expressed by

$$L_{\mathsf{p}}^{(\mathsf{sim})} = f(\lambda^{(\mathsf{D})}x)\;. \tag{4.3}$$

In Fig. 4, the results from simulation are juxtaposed to the theoretical decay envelope. The acoustic signal from CAA matches the theoretical damping envelope from Eq. (4.1) very well. The plot of the level decay of the rms-values within the computational domain is shown in Fig. 5. The computational results fit convincingly well the theoretical envelope along the range of $0.25\,\mathrm{m}$. With respect to technical application, this is a good result, as a typical installation depth is less. The prediction accuracy is comparable for a large frequency range. For the set of Linearized Perturbation Equations (LPE), the results (not shown) are nearly identical. Thus the implementation of the porous model is properly verified.

5. Conclusions

A set perturbation equations was presented predicting the emission and propagation of sound in the presence of both, free fluid and open type porous material. The first step, the Navier Stokes Equations (NS Equation) were volume averaged. This formal procedure leads to additional terms. All terms representing viscosity, heat conduction, subfilter stresses and entropy-modes were omitted in the context of sound propagation. The remaining terms are modeled by the Darcy and Forchheimer terms at the LHS of the momentum equation. Based on the physical idea of a finite averaging volume, continuous flow quantities were provided. The resulting set of governing equations was reformulated with intrinsically averaged primitive variables density and pressure. Further, a new Favre averaged velocity was defined, which is steady across the edge of free fluid and porous material.

In the next step, a decomposition of all variables into a steady meanflow and fluctuation was performed. Linearization of the fluctuating part led to the set of volume averaged Linearized Euler Equations (LEE). Reformulating the momentum equation and separation of all vorticity modes finally gave the set of Linearized Perturbation Equations (LPE). Main feature of the LPE is a vorticity source term at the RHS which must additionally be modeled by e.g. the Fast Random Particle Mesh Method (FRPM Method) refer to [17, 18], or analytic sources. The implementation of the new set of governing equation into the DLR PIANO-Code was verified with a test case. For different homogeneous, isotropic porous materials and different excitation frequencies, the damping

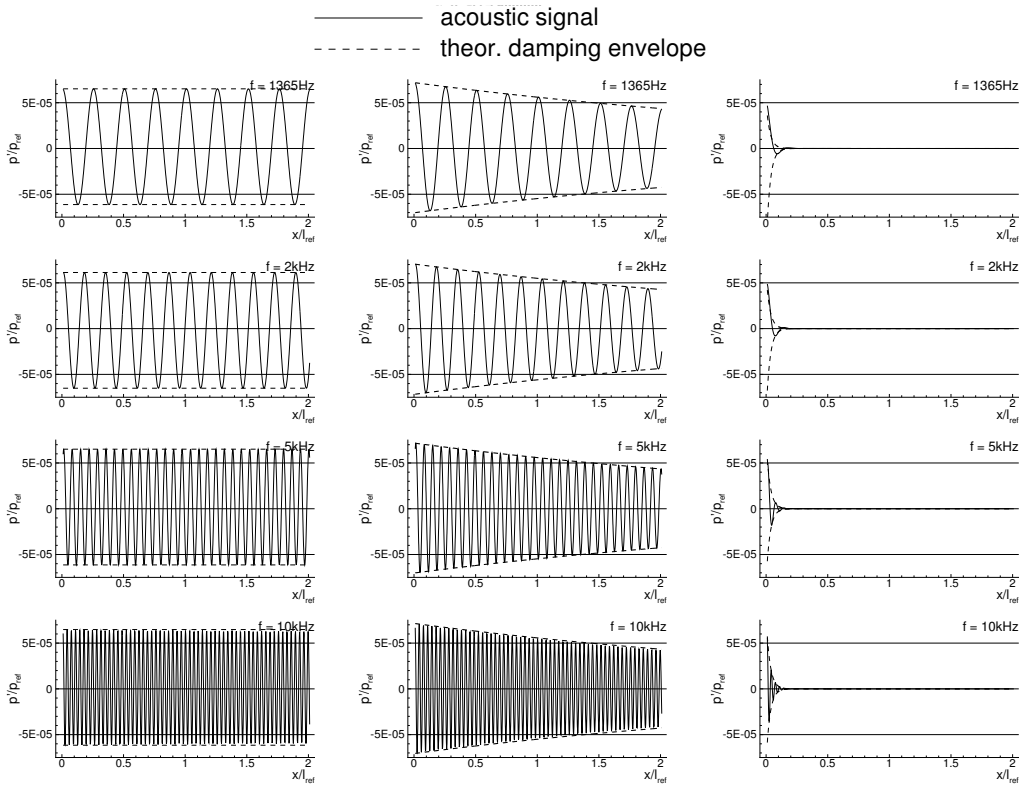

reference case:
$\phi\,\nu\,\kappa^{-1} = 0\,\frac{1}{\mathrm{s}}$

generic porosity:
$\phi\,\nu\,\kappa^{-1} = 1.715{\cdot}10^{2}\,\frac{1}{\mathrm{s}}$

realistic porosity:
$\phi\,\nu\,\kappa^{-1} = 22.649{\cdot}10^{3}\,\frac{1}{\mathrm{s}}$

FIGURE 4. Comparison of CAA results with Linearized Euler Equations (LEE) with theoretical damping envelope of the 1-D wave equation in a medium at rest from Eq. (4.1) for hisotropic, homogeneously porous materials with the Darcy constant $\phi\,\nu\,\kappa^{-1}$, [11].

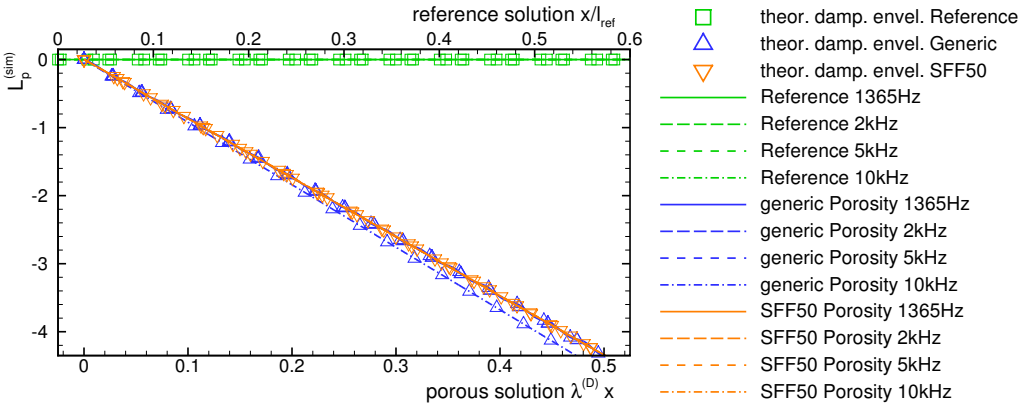

FIGURE 5. Comparison of CAA results with Linearized Euler Equations (LEE) with theoretical damping envelope of the 1-D wave equation in a medium at rest from Eq. (4.1) for isotropic porosity. For the reference case, the computational prediction is directly given, without comparison with the theoretical damping coefficient, what is $\lambda^{(\mathrm{D})} = 0$ for the free medium, [11].

behavior was compared to the analytical damping resulting from a modified wave equation. The solutions agree with the analytical solution for technically relevant penetration depths. In addition, proceeding validation of the porous model with a non-zero mean flow is presented in [19].

Acknowledgments

Financial support has been provided by the German Research Foundation (Deutsche Forschungsgemeinschaft – DFG) in the framework of the Sonderforschungsbereich 880. Computational resources have been provided by German Aerospace Center (Deutsches Zentrum für Luft- und Raumfahrt e.V., DLR), Institute of Aerodynamics and Flow Technology.

References

[1] RADESPIEL, R. AND HEINZE, W. (2014). SFB 880 – Fundamentals of High-Lift for Future Commercial Aircraft *CEAS Aeronautical Journal*, **5**(3), 1869–5582.

[2] HERR, M. (2007). Design Criteria for Low-Noise Trailing-Edges. *13th AIAA/CEAS Aeroacoustics Conference*, AIAA Paper **2007-3470**.

[3] HERR, M., ROSSIGNOL, K.-S., DELFS, J. W., MÖSSNER, M. AND LIPPITZ, N. (2014). Specification of Porous Materials for Low-Noise Trailing-Edge Applications *20th AIAA/CEAS Aeroacoustics Conference*, AIAA Paper **2014-3041**.

[4] POTT-POLLENSKE, M. (2014). LFF-Messungen mit DLR F15LS Modell im LuFo-Projekt MOVE.ON, Arbeitspaket LoNoSlat. *Personal Communication*.

[5] DELFS, J.W., BAUER, M., EWERT, R., GROGGER, H.A., LUMMER, M. AND LAUKE, T.G.W. (2008). Numerical Simulation of Aerodynamic Noise with DLR's aeroacoustic code PIANO *User Manual*, DLR.

[6] SLATTERY, J.C. (1969). Single-phase flow through porous media *AIChE Journal*, **15**(6), 866–872 .

[7] WHITAKER, S. (1973). The transport equations for multi-phase systems *Chemical Engineering Science*, **28**(1), 139–147.

[8] GRAY, W.G. AND LEE, P.C.Y. (1977). On the theorems for local volume averaging of multiphase systems *International Journal of Multiphase Flow*, **3**(4), 333–340.

[9] DREW, D.A. (1983). Mathematical Modeling of Two-Phase Flow *Annu. Rev. Fluid Mech.*, **15**(1), 261–291.

[10] CRIGHTON, D.G., DOWLING, A.P., FFOWCS WILLIAMS, J.E., HECKL, M.A. AND LEPPINGTON, F.A. (1996). Modern Methods in Analytical Acoustics: Lecture Notes, Springer Berlin.

[11] FASSMANN, B.W., RAUTMANN, C., EWERT, R. AND DELFS, J.W. (2015). Efficient prediction of broadband trailing edge noise and application to porous edge treatment *International Journal of Aeroacoustics, Special Issue Windenergy*, submitted.

[12] ASCHER, U.M., RUUTH, S.J. AND SPITERI, R.J. (1997). Implicit-Explicit Runge-Kutta methods for time-dependent partial differential equations *Applied Numerical Mathematics: Special Issue on Time Integration*, **25**(25), 151–167.

[13] BOSCARINO, S. AND RUSSO, G. (2007). On the uniform accuracy of IMEX Runge-Kutta schemes and applications to hyperbolic systems with relaxation In: Luigia Puccio*Communications to SIMAI Congress*, Messima, Italy.

[14] EWERT, R., BAUER, M. AND LUMMER, M. (2012). A Review of State-of-the-Art Aeroacoustic Prediction Approaches In: Schram, C. and Dénos, R.*Aircraft noise*, Von Karman Institute for Fluid Dynamics, Rhode Saint Genèse, Belgium.

[15] THOMPSON, K.W. (1987). Time dependent boundary conditions for hyperbolic systems , **68**(1), 1–24.

[16] THOMPSON, K.W. (1990). Time-dependent boundary conditions for hyperbolic systems, II *Journal of Computational Physics*, **89**(2), 439–461.

[17] EWERT, R. (2008). Broadband slat noise prediction based on CAA and stochastic sound sources from a fast random particle-mesh (RPM) method *Turbulent Flow and Noise Generation*, **37**(4), 369–387

[18] EWERT, R., DIERKE, J., SIEBERT, J., NEIFELD, A., APPEL, C., SIEFERT, M. AND KORNOW, O. (2011). CAA broadband noise prediction for aeroacoustic design *Journal of Sound and Vibration*, **330**(17), 4139–4160

[19] FASSMANN, B.W., RAUTMANN, C., EWERT, R. AND DELFS, J.W. (2015). Prediction of Porous Trailing Edge Noise Reduction via Volume Averaged Linearized Perturbation Equations *AIAA Aviation Forum 2015*, submitted.